

Invasion-wave induced first-order phase transition in systems of active particles

Thomas Ihle¹

¹*Department of Physics, North Dakota State University, Fargo, North Dakota, 58108-6050, USA*

An Enskog-like kinetic equation for self-propelled particles is solved numerically. I study a density instability near the transition to collective motion and find that while hydrodynamics breaks down, the kinetic approach leads to soliton-like supersonic waves with steep leading kinks and Knudsen numbers of order one. These waves show hysteresis, modify the transition threshold and lead to an abrupt jump of the global order parameter if the noise level is changed. Thus they provide a mechanism to change the second-order character of the phase transition to first order.

Collective motion of self-propelled agents is a key feature of active matter systems and has attracted much attention [1–3]. Systems of interest range from animal flocks [4], to human crowds [5], actin networks driven by molecular motors [6], interacting robots [7], and mixtures of robots and living species [8].

Most of our theoretical understanding of collective motion comes from two sources: (i) computational studies of particle-based models and (ii) phenomenological transport equations which are usually postulated by means of symmetry arguments as in the seminal work by Toner and Tu [9, 10]. These authors showed that even in a two-dimensional system, long-range orientational order is possible due to the nonzero speed of the particles. Many of the computational approaches [11–20] are related to the minimal Vicsek-model (VM) [21]. In the VM, point-like particles move at fixed speed and try to align locally with their neighbors but do not succeed completely due to the presence of some noise. As the noise amplitude decreases, the system experiences a phase transition from a disordered state, in which the particles have no preferred global direction, to an ordered state, in which, on average, the particles move in the same direction.

This paper is based on a third angle of attack – the kinetic theory of gases. Apart from a few exceptions [22–24] the kinetic approach to active particle systems has been less popular. However, it is very powerful and allowed the solution of a long standing problem, the rigorous derivation of the hydrodynamic theory for the VM [26]. See also Refs. [32–34] for alternative derivations.

Direct simulations of the VM [11, 12, 36] revealed that right at the onset of ordered motion, large density waves emerge. It has been intensely debated [11–13, 21, 36] whether this order-disorder transition is continuous or discontinuous. By now it is generally accepted that at high particle speeds the transition is discontinuous with strong finite size effects. This is in puzzling contrast to mean-field theories [24–28] which should be valid at large speeds but predict a continuous transition.

In this Letter, I show that the solution of this puzzle lies beyond hydrodynamic theory. I find that a special soliton-like density wave, which can be analyzed by kinetic theory but not by hydrodynamics, is able to alter the character of the phase transition from continuous to

discontinuous. I calculate the global order parameter for collective motion and show explicitly how its hysteresis and its unique finite size effects are related to the properties of the density waves.

The reason why these waves escape hydrodynamic treatment is that they violate a basic principle for the validity of a hydrodynamic theory – the smallness of the Knudsen number – which requires that the average distance particles travel between collisions is much smaller than the length over which hydrodynamic fields change considerably. This is not true for the waves emerging near the onset of collective motion. They are so steep that their Knudsen number is always of order one.

In one of the first analytical studies of active particles, Bertin *et al.* [24, 25] have also analyzed soliton waves. However, the calculated density profiles (Fig. 7 of Ref. [25]) bear little resemblance with the actual profiles obtained in direct simulations of the VM, which have a very sharp leading edge. Gopinath *et al.* [30] also calculated waves which look different from the ones observed in simulations. Both groups obtained waves *within* the hydrodynamic approach and did not observe that the waves have any effect on the order-disorder threshold. The waves calculated in this Letter by means of kinetic theory are qualitatively different from the ones of Refs. [25, 30] because (i) they shift the transition threshold and modify the character of the flocking transition from second to first-order, and (ii) their profile semi-quantitatively agrees with the ones measured in direct simulations [31].

A first clue about the inadequacy of hydrodynamic equations for the VM comes from Ref. [26] where it was shown that if all coefficient in these equations are rigorously derived from the microscopic dynamics, long wavelength density modulations evolve into waves with infinite amplitudes. Thus, contrary to Refs. [25, 30] no solitons could be found. The equations were derived under the assumption that higher order gradient terms are negligible which is not justified when steep spatial perturbations of a homogeneous state grow sufficiently large. Usually, such perturbations are stabilized by higher order nonlinear terms. This is not the case here, the hydrodynamic equations are driven out of their range of validity. To discover the final fate of these waves within the hydrodynamic approach one would have to explicitly sum gra-

dent terms of all orders, which is practically impossible. I circumvent this obstacle by abandoning hydrodynamics entirely. Instead, I numerically solve the space and time-dependent kinetic equations of the VM. Because this does not involve any gradient expansion, a summation to all orders is achieved implicitly.

In the VM, N pointlike particles with positions $\mathbf{x}_i(t)$ and velocities $\mathbf{v}_i(t)$ undergo a discrete-time dynamics with time step τ . The evolution consists of two steps: streaming, where all positions are updated according to $\mathbf{x}_i(t + \tau) = \mathbf{x}_i(t) + \tau\mathbf{v}_i(t)$, and collision. The magnitude v_0 of the particle velocities is kept constant, only the directions θ_i of the velocity vectors are modified in the collision step: a circle of radius R is drawn around a given particle and the average direction Φ_i of motion of the particles within the circle is determined according to $\Phi_i = \arctan[\sum_j^n \sin(\theta_j)/\sum_j^n \cos(\theta_j)]$. The new directions follow as $\theta_i(t + \tau) = \Phi_i(t) + \xi_i$. Here, ξ_i is a random number which is uniformly distributed in the interval $[-\eta/2, \eta/2]$.

Following Ref. [26], the time evolution of the VM can be described by a Markov chain for the N -particle probability density. This equation is exact but intractable without simplification. The easiest way to proceed is to make Boltzmann's molecular chaos approximation and assume that the particles are uncorrelated *prior* to a collision, which amounts to a factorization of the N -particle probability into a product of one-particle probabilities. Because this assumption neglects correlations and leads to an effective one-particle picture, it can be thought of as a sort of mean-field theory which looks like an Enskog equation,

$$\begin{aligned} f(\theta, \mathbf{x}, t + \tau) &= \frac{1}{\eta} \int_{-\eta/2}^{\eta/2} d\xi \sum_{n=1}^N \frac{1}{(n-1)!} e^{-M_R(\mathbf{x}', t)} \\ &\times \int_0^{2\pi} d\tilde{\theta}_1 \left[\prod_{i=2}^n \int_0^{2\pi} d\tilde{\theta}_i \int_{\odot} d\tilde{\mathbf{x}}_i f(\tilde{\theta}_i, \tilde{\mathbf{x}}_i, t) \right] \\ &\times f(\tilde{\theta}_1, \mathbf{x}', t) \hat{\delta}(\theta - \xi - \Phi_1(\tilde{\theta}_1, \dots, \tilde{\theta}_n)). \end{aligned} \quad (1)$$

The distribution function $f(\theta, \mathbf{x})$ is proportional to the probability to find a particle with a given angle θ at location \mathbf{x} . Details on this derivation can be found in Refs. [26, 35, 40]. The r.h.s. of Eq. (1) is the collision integral and will be denoted as $I[f]$. It is a nonlinear functional of the distribution function with a singular kernel which consists of the periodically continued Dirac-delta function, $\hat{\delta}(\alpha) = \sum_{m=-\infty}^{\infty} \delta(\alpha + 2\pi m)$. The argument of the exponential in Eq. (1), $M_R(\mathbf{x}', t) = \int_{\odot} \rho(\mathbf{y}, t) d\mathbf{y}$, is the average number of particles in a circle of radius R centered around $\mathbf{x}' = \mathbf{x} - \mathbf{v}\tau$ where $\mathbf{v} = v_0(\cos\theta, \sin\theta)$ is a velocity vector. This interaction circle is not centered around the final position \mathbf{x} because after the reference particle $i = 1$ has collided with particles $2, 3 \dots n$ it will be convected to location \mathbf{x} in the subsequent streaming step. The symbol \odot denotes spatial integra-

tions over the collision circle. The particle density ρ is given as the zeroth moment of the distribution function, $\rho(\mathbf{x}, t) = \int_0^{2\pi} f(\theta, \mathbf{x}, t) d\theta$.

Eq. (1) is solved by an algorithm which is related to the Lattice-Boltzmann method (LB) [41]. It relies on a set of Q microscopic velocities, \mathbf{e}_i , where every velocity is associated with a distribution function $f_i(\mathbf{x}, t)$. The positions \mathbf{x} are discretized on a regular lattice of size $L_x \times L_y$. See Supplemental Material at [URL] for details on this numerical method. In contrast to LB a very large number of velocities, $Q \approx 1000$, is used to accurately resolve the order-disorder transition. Another difference is the nonlocal collision term $I[f]$ which requires spatial and angular integrations. Naive attempts to calculate $I[f]$ by a simple integration scheme lead to prohibitively slow performance. A much more accurate and faster way is to evaluate the collision integral in angular Fourier space. Expanding f ,

$$f(\theta, \mathbf{x}) = \sum_{k=0}^{k_C} [g_k(\mathbf{x}) \cos(k\theta) + h_k(\mathbf{x}) \sin(k\theta)], \quad (2)$$

performing a similar expansion for $I[f]$, and evaluating Eq. (1) in this basis gives a simple set of algebraic relations for the Fourier coefficients of the collision integral in terms of g_k and h_k , see Eq. (S2) in the Supplemental Material at [URL]. Three-particle and higher order collisions have been neglected. While this restriction to binary interactions keeps the simulation times short and reduces the validity of the numerics to low densities, $M_R < 1$, it is not a principal limitation. Similar to Ref. [35], the algorithm can be easily extended to include genuine three-, and higher particle collisions. In Eq. (2) all angular modes with wavenumbers k larger than the cut-off value $k_C = 5$ were neglected. The remaining modes are sufficient to describe the behavior of the order parameter in the vicinity of a phase transition. The global order parameter Ω is defined by means of the $k = 1$ Fourier coefficients, $\Omega = \langle \sqrt{g_1^2 + h_1^2} \rangle$ where the brackets denote an average over the simulation box. These coefficients are proportional to the components of the momentum density \mathbf{w} , $g_1 \propto w_x$, $h_1 \propto w_y$, which is given by the first moment of the distribution function, $\mathbf{w}(\mathbf{x}, t) = \int_0^{2\pi} \mathbf{v}(\theta) f(\theta, \mathbf{x}, t) d\theta$.

Let us first consider a very small system, $L_x = L_y = 4$ with periodic boundary conditions and average particle density $\rho_0 = N/(L_x L_y) = 0.00424$. To initialize a disordered state, all angular Fourier coefficients except $g_0 = \rho_0/2\pi$ are set to zero. In this and all following simulations, the average particle number in the collision circle, $M = \pi R^2 \rho_0$, is set to $M = 0.03$ and the time step is $\tau = 1$. Recently [26], the critical noise η_C as a function of M has been calculated. By choosing a noise value $\eta = 0.43$ slightly smaller than the threshold value $\eta_C = 0.4361$, the system is quenched into the ordered state. Since the system size is much smaller than the

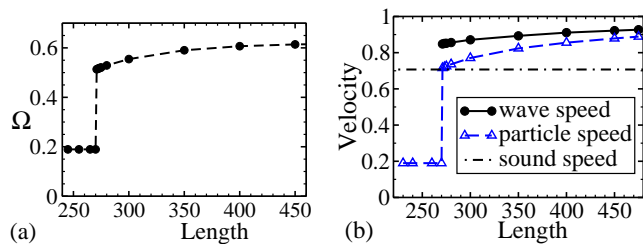


FIG. 1. (a) Steady state order parameter Ω ; (b) speed of the invasion wave v_W (circles) and average particle speed $u = |\mathbf{w}|/\rho$ (triangles) measured at the tip of the wave versus system size. The dash-dotted line shows the speed of sound in the disordered phase, $v_S = v_0/\sqrt{2}$. All speeds are plotted

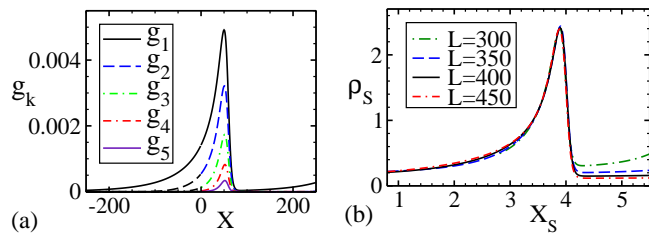


FIG. 2. (a) The Fourier coefficients g_k for a stationary invasion wave travelling into the positive x -direction as a function of position. (b) The rescaled density $\rho_S = \rho L_x^{-2} 10^6$ versus rescaled position $X_S = x L_x^2 10^{-5}$ for different system sizes. Parameters are the same as in Fig. 1.

critical length $L_0 = 2\pi/k_0$ (see Fig. 2 of [26]) above which the homogeneous ordered state is linearly unstable, the system is expected to stay homogeneous. The numerical solution of Eq. (1) agrees with these predictions: the zero momentum disordered state evolves into a stable ordered state. As shown in Fig. 1(a), the order parameter stays constant at increasing system size until a critical size of $L^* \approx 270.5$ is reached. When the system size is adjusted by just one lattice unit from $L = 270$ to 271, Ω makes an abrupt jump, almost tripling its value. A closer look reveals that while the steady state solution is homogeneous at small L , it is not homogeneous above L^* . Instead, a single-peaked density wave is going through the system. It travels at constant velocity v_W and, as seen in Fig. 2, has a pronounced asymmetric shape with a steep front and an extended tail. The anharmonicity of this shape, together with previous results [26], provide a simple explanation for the discontinuity of the global order parameter: The wave is born as a result of a linear instability and inherent noise. Once it exists, it grows to a large final size because nonlinear attenuation is ineffective. The definition of Ω involves a spatial average which is dominated by the extended spatial region behind the peak of the wave, where local order is much stronger than in the corresponding homogeneous ordered state. Even though the area ahead of the wave front is mostly disordered with $|\mathbf{w}| \approx 0$, it cannot compensate the huge contributions to Ω from the densest part of the wave. As a result of this biased average, the global order param-

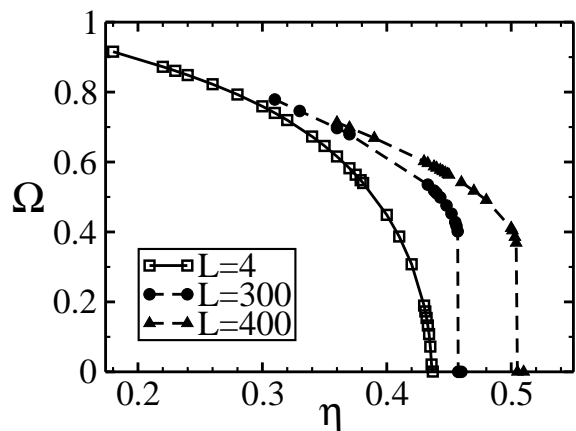


FIG. 3. Order parameter versus noise η for several system sizes L . Parameters: $R = 0.1$, $v_0 = 1$.

ter is much larger than in the homogeneous ordered state. These waves have remarkable properties. For example, Fig. 1(b) shows that their speed v_W is just slightly below the maximum possible speed v_0 , but larger than the speed of sound in the disordered phase, $v_S = v_0/\sqrt{2}$. The waves are always supersonic with Mach numbers between 1.19 and 1.41. The particles at the highest (that is densest) point of the wave are so strongly aligned that their average speed $u = |\mathbf{w}|/\rho$ is only slightly less than v_W . Thus, most particles in the wave crest travel with the wave and do not just undergo restricted local motion. The particles just ahead of the wave front have low density and display disordered motion. They do not “feel” the wave coming since it arrives faster than the speed of sound. Their territory is invaded and a fraction of them becomes strongly aligned and joins the wave for a while. This motivates the term *invasion wave*.

In agreement with direct simulations [37], I observe that the invasion wave has a perfectly straight front, perpendicular to its direction of motion. To accelerate the numerics, I take advantage of this apparent one-dimensional nature and drastically reduce the y -extension of the box to $L_y = 2$, creating a very elongated simulation box. Examining large box lengths L_x , one realizes that the maximum density in a wave and the steepness of the leading edge depends on system size in a very sensible way that transcends the traditional meaning of “finite size effects”. In particular, the maximum density in the wave is proportional to L_x^2 , and the width of the peak scales as $1/L_x^2$. In fact, the invasion wave cannot be seen as a localized perturbation of some mainly undisturbed medium. It is rather a global excitation of the entire system where, facilitated by periodic boundary conditions, all parts of the system are involved and particles everywhere adjust accordingly. In Fig 2(b), by scaling the x -coordinate by L_x^{-2} and the density by L_x^2 it is demonstrated that here is a master curve for the shape of an invasion wave. As a consequence, the maximum density gradient at the leading edge is proportional to

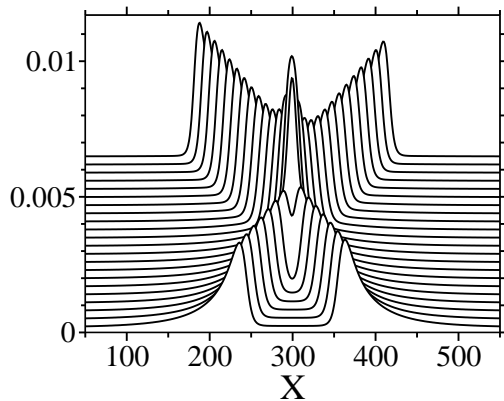


FIG. 4. Snapshots for the head-on collision of two soliton-like waves. The sequence starts with two well separated peaks close to the x-axis running towards collision with their steep fronts facing each other. At the latest time, the peaks are separated again after a successful “tunneling” through each other and now run towards the edges of the box.

L_x^4 . To understand why these waves have not been detected by means of hydrodynamic approaches [25, 30] an effective Knudsen number, $Kn = \lambda/r$ is defined. Here, $\lambda = v_0\tau$ is the mean free path of a particle and r is the radius of curvature of the density profile at the tip of the wave. It turns out that Kn is never smaller than about $1/2$, not even in the smallest systems that allow wave formation. At such Knudsen numbers, a structure with a small internal scale moves quite a large distance in one time step, causing hydrodynamic gradient expansions to diverge.

Assuming a homogeneous ordered state, the mean-field theory of the VM [26] predicts that the flocking transition is continuous. To check whether this is still true for inhomogeneous ground states, I calculate the order parameter as a function of noise for different system sizes. According to Fig. 3, at the smallest size $L = 4$ where the system is still homogeneous, a continuous transition occurs. However, in bigger systems, very close to the predicted threshold $\eta_C = 0.4361$, Ω still has a large value because of persistent waves. To accurately establish the order of this transition I used the following simulation protocol: An ordered state with a stable stationary wave at very low noise η_0 is created. This inhomogeneous state serves as initial condition for a run with slightly larger noise $\eta_1 > \eta_0$. After convergence, the noise is increased again. This way, a sequence of stable inhomogeneous states with large order parameters is obtained, even at noise values a few percent above η_C . Approaching the threshold from the higher noise side confirms that the disordered state with $\Omega = 0$ is stable for $\eta \geq \eta_C$. Hence, the flocking transition shows hysteresis; the wave state can coexist with the homogeneous state over a finite noise range $\Delta\eta \approx 0.045\eta_C$ for $L = 300$. This concludes the proof for the discontinuity of the order-disorder transition for large L , at the mean-field level. As seen in Fig.

3 the hysteresis region grows with system size because the properties of the underlying soliton-like wave strongly depends on L . Compared to equilibrium systems, the phase behavior depicted in Fig. 3 looks unusual. Nevertheless, it semi-quantitatively agrees with direct simulations of the VM [38, 39].

One of the defining properties of a soliton is the ability to pass through each other without destruction. To perform this “soliton test”, I prepared stationary waves in two different systems with slightly different sizes, $L_x = 299$ and $L_x = 300$ and ensured they run in opposite directions. After the waves became stationary, I “glued” the two boxes together leading to a longer system with $L_x = 599$. A series of snapshots of the time evolution of this two peak system is shown in Fig. 4. At the earliest time one sees two peaks running towards each other. Eventually, they start to overlap and form a large single peak. A while later, the two peaks reemerge with almost undisturbed shape like a conventional soliton. Watching the time evolution through repeated collisions reveals that if the waves have a tiny height difference initially, this difference is amplified in every encounter. The bigger soliton takes a few particles away from the smaller one in every meeting until only one peak survives. Gradual coarsening also occurs inbetween collisions or when waves travel in the same direction. Therefore, true stationary states have only one peak.

In conclusion, using kinetic theory I analyzed supersonic waves that occur in the Vicsek model once the system exceeds a critical size. I demonstrated that the waves show hysteresis and alter the order of the flocking transition from continuous to discontinuous. A phase diagram with atypical finite size effects was calculated. I argue that these waves were probably not detected in previous analytical approaches because of their large Knudsen number. This provides an explicit example of an active particle model where hydrodynamic equations fail to correctly describe one of the most important properties – the nature of the phase transition. This could have implications for other, more sophisticated, models of active matter. While my calculations neglect correlations which are relevant at small particle speeds, they do demonstrate a novel mechanism to induce a first-order flocking transition. How relevant this mechanism is in the low speed regime and for particles with nonzero size remains an open question. I speculate that some aspects of this approach remain useful. For example, it might lay the ground for a theory in terms of interacting quasi-particles that represent soliton waves.

Support from the National Science Foundation under grant No. DMR-0706017 is gratefully acknowledged.

-
- [1] S. Ramaswamy, *Annu. Rev. Condens. Matter Phys.* **1**, 323 (2010).
- [2] T. Vicsek and A. Zafeiris, *Phys. Rep.* **517**, 71 (2012).
- [3] M.C. Marchetti *et al.*, arXiv:1207.2929, (2012).
- [4] J.K. Parrish and L. Edelstein-Keshet, *Science* **284**, 99 (1999); I.D. Couzin *et al.*, *Nature* **433**, 513 (2005); I.D. Couzin, J. Krause, *Adv. Stud. Behav.* **32**, 1 (2003); R.W. Tegeeder, J. Krause, *Philos. Trans. R. Soc. London B* **350**, 381 (1995); N. Abaid, M. Porfiri, *J. R. Soc. Interface* **7** 1441 (2010).
- [5] D. Helbing, I. Farkas, T. Vicsek, *Nature* **407**, 487 (2000); D. Helbing, *Rev. Mod. Phys.* **73**, 1067 (2001).
- [6] V. Schaller *et al.*, *Nature* **467**, 73 (2010); V. Schaller, C. Weber, E. Frey and A.R. Bausch, *Soft Matt.* **7**, 3213 (2011); J. F. Joanny *et al.*, *New J. Phys.* **9** 422 (2007).
- [7] A. Jadbabaie, J. Lin, S. Morse, *IEEE Trans. Auto. Control* **48**, 988 (2003); A.E. Turgut *et al.*, *Swarm Intell.* **2**, 97 (2008); W.M. Shen *et al.* *Auton. Robots* **17**, 93 (2004).
- [8] R. T. Vaughan *et al.*, *Robot. Auton. Syst.* **31**, 109 (2000); J. Halloy *et al.*, *Science* **318**, 1155 (2007); S. Marras, M. Porfiri, *J. R. Soc. Interface* **9**, 1856 (2012).
- [9] J. Toner and Y. Tu, *Phys. Rev. Lett.* **75**, 4326 (1995); *Phys. Rev. E* **58**, 4828 (1998).
- [10] J. Toner, *Phys. Rev. E* **86**, 031918 (2012).
- [11] G. Grégoire and H. Chaté, *Phys. Rev. Lett.* **92** 025702 (2004); *Phys. Rev. Lett.* **99**, 229601 (2007); *Eur. Phys. J. B* **64** 451 (2008).
- [12] H. Chaté, F. Ginelli, G. Grégoire, F. Raynaud, *Phys. Rev. E* **77** 046113 (2008);
- [13] G. Baglietto, E.V. Albano, *Phys. Rev. E* **78**, 021125 (2008); *Phys. Rev. E* **80**, 050103 (2009).
- [14] F. Ginelli *et al.*, *Phys. Rev. Lett.* **104** 184502 (2010);
- [15] F. Peruani *et al.*, *J. Phys. Conf. Ser.* **297** 012014 (2011).
- [16] H. Levine, W.-J. Rappel, I. Cohen, *Phys. Rev. E* **63**, 017101 (2000).
- [17] V. Dossetti, F.J. Sevilla, V.M. Kenkre, *Phys. Rev. E* **79**, 051115 (2009).
- [18] F. Ginelli, H. Chaté, *Phys. Rev. Lett.* **105**, 168103 (2010).
- [19] V. Lobaskin, M. Romenskyy, *Eur. Phys. J. B* **86**, 91 (2013).
- [20] M. Meschede, O. Hallatschek, arXiv:1212.2060v1 (2012).
- [21] T. Vicsek *et al.*, *Phys. Rev. Lett.* **75**, 1226 (1995); A. Czirók, H. E. Stanley, T. Vicsek, *J. Phys. A*, **30**, 1375 (1997); M. Nagy, I. Daruka, T. Vicsek, *Physica A* **373**, 445 (2007).
- [22] D. Helbing, *Phys. Rev. E* **53**, 23662381 (1996).
- [23] H.J. Bussemaker, A. Deutsch, and E. Geigant, *Phys. Rev. Lett.* **78**, 5018 (1997).
- [24] E. Bertin, M. Droz, and G. Grégoire, *Phys. Rev. E* **74**, 022101 (2006).
- [25] E. Bertin, M. Droz, and G. Grégoire, *J. Phys. A* **42**, 445001 (2009).
- [26] T. Ihle, *Phys. Rev. E* **83**, 030901 (2011).
- [27] J.A. Pimentel *et al.*, *Phys. Rev. E* **77** 061138 (2008).
- [28] M. Aldana, C. Huepe, *J. Stat. Phys.* **112**, 135 (2003).
- [29] M. Aldana *et al.*, *Phys. Rev. Lett.* **98**, 095702 (2007).
- [30] A. Gopinath *et al.*, *Phys. Rev. E* **85**, 061903 (2012).
- [31] See Fig. 13(d) in Ref. [12] and Fig. 8(c) in [25].
- [32] P. Romanczuk, L. Schimansky-Geier, *Ecol. Complex.* **10**, 83 (2012).
- [33] R. Großmann, L. Schimansky-Geier, P. Romanczuk, arXiv:1301.5890v2 (2013).
- [34] S. Mishra, A. Baskaran, M.C. Marchetti, *Phys. Rev. E* **81**, 061916 (2010).
- [35] Y.-L. Chou, R. Wolfe, T. Ihle, *Phys. Rev. E* **86** 021120 (2012).
- [36] M. Aldana, H. Larralde, B. Vazquez, *Int. J. Mod. Phys. B* **23** 3661 (2009).
- [37] See Fig. 13 in Ref. [12] and Fig. 8 in [25].
- [38] See Fig. 2(a) in Ref. [12] and Fig. A1(b) in [25].
- [39] G. Baglietto (2013), private communication.
- [40] T. Ihle, *Phys. Chem. Chem. Phys.* **11**, 9667 (2009).
- [41] X. He, L-S. Luo, *Phys. Rev. E* **56**, 6811 (1997); S. Chen, G.D. Doolen, *Ann. Rev. Fluid Mech.* **30**, 329 (1998).